

AD-786 578

GAMMA-IRRADIATION DAMAGE IN AGE  
HARDENING AL ALLOYS

Nicholas F. Fiore

Notre Dame University

Prepared for:

Ballistic Research Laboratories

July 1974

DISTRIBUTED BY:

**NTIS**

National Technical Information Service  
U. S. DEPARTMENT OF COMMERCE  
5285 Port Royal Road, Springfield Va. 22151

BRL CR 167

# BRL

AD

AD 786578

CONTRACT REPORT NO. 167

GAMMA-IRRADIATION DAMAGE IN AGE  
HARDENING AL ALLOYS

Prepared by

University of Notre Dame  
Department of Metallurgical Engineering  
and Materials Science  
Notre Dame, Indiana

July 1974

DDC  
OCT 1 1974  
RECEIVED

Approved for public release; distribution unlimited.

USA BALLISTIC RESEARCH LABORATORIES  
ABERDEEN PROVING GROUND, MARYLAND

ib

As ordered by  
NATIONAL TECHNICAL  
INFORMATION SERVICE  
U.S. Department of Commerce  
Springfield, VA 22151

43

Destroy this report when it is no longer needed.  
Do not return it to the originator.

Secondary distribution of this report by originating  
or sponsoring activity is prohibited.

Additional copies of this report may be obtained  
from the National Technical Information Service,  
U.S. Department of Commerce, Springfield, Virginia  
22151.

ACCESSION for	
NTIS	White Section <input checked="" type="checkbox"/>
DDO	Blue Section <input type="checkbox"/>
USC & AFM	<input type="checkbox"/>
JUSTIN	
BY	
OF SECTION/AVAILABILITY CODES	
DISC	Avail. Code
A	

The findings in this report are not to be construed as  
an official Department of the Army position, unless  
so designated by other authorized documents.

ic

UNCLASSIFIED

SECURITY CLASSIFICATION OF THIS PAGE (When Data Entered)

REPORT DOCUMENTATION PAGE		READ INSTRUCTIONS BEFORE COMPLETING FORM
1. REPORT NUMBER CONTRACT REPORT NO. 167	2. GOVT ACCESSION NO.	3. RECIPIENT'S CATALOG NUMBER <b>AD-786578</b>
4. TITLE (and Subtitle) GAMMA-IRRADIATION DAMAGE IN AGE HARDENING AL ALLOYS		5. TYPE OF REPORT & PERIOD COVERED FINAL
		6. PERFORMING ORG. REPORT NUMBER
7. AUTHOR(s) Nicholas F. Fiore		8. CONTRACT OR GRANT NUMBER(s) DAAD05-70-C-0085
9. PERFORMING ORGANIZATION NAME AND ADDRESS University of Notre Dame Dept of Metallurgical Eng & Materials Science Notre Dame, Indiana 46556		10. PROGRAM ELEMENT, PROJECT, TASK AREA & WORK UNIT NUMBERS RDT&E 1T061102A33E
11. CONTROLLING OFFICE NAME AND ADDRESS U.S. Army Ballistic Research Laboratories Aberdeen Proving Ground, Maryland 21005		12. REPORT DATE JULY 1974
		13. NUMBER OF PAGES
14. MONITORING AGENCY NAME & ADDRESS (if different from Controlling Office)		15. SECURITY CLASS. (of this report) UNCLASSIFIED
		15a. DECLASSIFICATION/DOWNGRADING SCHEDULE
16. DISTRIBUTION STATEMENT (of this Report) Approved for public release; distribution unlimited.		
17. DISTRIBUTION STATEMENT (of the abstract entered in Block 20, if different from Report)		
18. SUPPLEMENTARY NOTES Details of illustrations in this document may be better studied on microfiche		
19. KEY WORDS (Continue on reverse side if necessary and identify by block number) Gamma Irradiation Damage Aluminum Alloys Internal Friction Electron Microscopy		
20. ABSTRACT (Continue on reverse side if necessary and identify by block number) Pure Al and a series of age-hardenable Al alloys have been $\gamma$ -irradiated in a $\text{Co}^{60}$ source at a dose of $6 \times 10^3$ rads/min. Internal friction measurements have been made at 80 kHz by means of the Marx technique on samples <u>in situ</u> during irradiation. In Al and Al-3 w/o Cu, the damping decreases monotonically as is expected. The decrease is attributed to the immobilization of dislocations by the radiation- induced point defect pinners. In 2024-T6, 2017-T6 and Al-9.5 Mg, the damping		

DD FORM 1473 1 JAN 73 EDITION OF 1 NOV 68 IS OBSOLETE

UNCLASSIFIED

SECURITY CLASSIFICATION OF THIS PAGE (When Data Entered)

UNCLASSIFIED

SECURITY CLASSIFICATION OF THIS PAGE (When Data Entered)

Block 20. (cont'd)

passes through a minimum and begins an anomolous increase after 4 to 7 hours of irradiation.

Electron micrographs show that in Al and Al-3 w/o Cu, irradiation does not influence structure. In the alloys which display the damping minimum however, precipitate morphology changes during irradiation, with coarsening and/or de-coarsening and re-nucleation being observed.

The effect appears to depend upon the presence of Mg. Theory predicts that morphology changes can occur during  $\gamma$ -irradiation, with the mechanism being either Rutherford collision or Coulombic repulsion radiation damage.

ia

UNCLASSIFIED

SECURITY CLASSIFICATION OF THIS PAGE (When Data Entered)

## TABLE OF CONTENTS

INTRODUCTION.....	1
LITERATURE SURVEY.....	3
$\gamma$ -Irradiation Damage Through Rutherford Collisions.....	3
Rutherford Collision Damage in Multiphase Alloys.....	6
Coulombic Repulsion Damage in Multiphase Alloys	10
EXPERIMENTAL RESULTS.....	13
Damping Studies of Precipitation in Al-Cu.....	13
Irradiation-Damping Studies.....	16
CONCLUSIONS.....	21
The Existence of an Effect.....	21
Mechanisms of the Effect.....	22
Property Control in a $\gamma$ -Irradiation Environment.	22

## INTRODUCTION

Prior to about 1970, the literature on radiation damage in metals could be divided into two broad categories. One consisted of reports of basic damage mechanisms in pure metals and single phase alloys. The other consisted of empirical, rather than mechanistic studies of the properties of multi-phase engineering alloys. Consequently, most theoretical analyses of radiation damage mechanisms were based on data on materials which could not be used as structural components in a radiation environment.

The simple empirical documentation of properties of actual engineering materials has become inadequate as the nuclear environment has become more hostile e.g. in the fast breeder reactor. It has become necessary to understand materials' response to radiation so that selection and processing might be optimized.

An obvious example of the application of basic studies of damage in commercial materials is the investigation of swelling behavior of austenitic stainless steel fuel element cladding. Detailed theoretical modeling<sup>1</sup> based on thermodynamics and kinetics and rather refined transmission electron microscopy<sup>2</sup> analyses of defects have characterized the study. Recently the mechanistic approach has been extended to precipitation-hardenable Ni-base superalloys<sup>3</sup> since these multiphase materials appear to resist swelling more effectively than the stainless steels.

This report describes an experimental program directed toward an understanding of the mechanisms of  $\gamma$ -irradiation damage in another class of useful materials, precipitation-hardenable Al alloys. The potential engineering significance of this basic study is pointed out in Figure 1, which shows room-temperature

Charpy impact strength of alloy 2017, heat-treated to the fully-strengthened T6 condition. As the hardened alloy is  $\gamma$ -irradiated in a  $\text{Co}^{60}$  cell, a noticeable decrease in toughness is apparent. The trend, with each point representing the average of five tests, indicates that irradiation must influence structure since it influences properties. Gamma-irradiation is normally considered a rather mild radiation environment, so this suggests that it is dangerous to neglect it as being capable of influencing material behavior. It further suggests that intense neutron doses are not the only type of environment whose damage mechanisms must be understood.

The research program is directed toward answering several questions about the effect observed in Figure 1.

1. Is the effect real?
2. If it is real, what are the mechanisms of the structural changes causing property changes?
3. How can these mechanisms be controlled so as to guarantee the satisfactory performance of these materials in a  $\gamma$  or electron irradiation environment?



## LITERATURE SURVEY

### $\gamma$ -Irradiation Damage Through Rutherford Collisions

The extent of crystalline damage caused by neutron, proton, or heavy-ion irradiation is enormous relative to that caused by direct electron or  $\gamma$  (indirect-electron) irradiation. Heavier particles cause long tracks of displaced atoms in the form of vacancies and interstitials, voids, and dislocation loops. This damage so overshadows that done by electrons that it is usually reasonable to neglect  $\gamma$  or electron irradiation as playing a role in influencing microstructure. As more evidence of morphology change from electron and  $\gamma$ -irradiation becomes available, the danger of this neglect becomes evident.

The solid state physicist and materials scientist usually think of radiation damage occurring because of Rutherford or "billiard ball" collisions between high energy particles and nuclei. An incoming particle transfers its momentum to an atom on a lattice site, displacing it and thereby causing crystal damage. The literature survey begins with a summary of this damage mechanism, although subsequent discussion will show that Rutherford collisions may not be the only relevant damage mechanism in multiphase alloys.

Of the multitude of references on  $\gamma$ -irradiation in metal crystals, the book by Chadderton<sup>4</sup> and the review by Sosin<sup>5</sup> present particularly complete treatments of the inter-relation between radiation absorption and crystal defect structure.

Chadderton points out that  $\gamma$ -rays may be absorbed and cause radiation damage by a number of processes. In the  $\gamma$ -energy range between 0.5 and 5 MeV, however, practically all absorption and damage in metals is caused by Compton electrons.<sup>6</sup> In the

Compton effect a  $\gamma$ -quantum strikes a free electron, transferring a portion of its kinetic energy (momentum) and causing the electron to move as a charged particle through the lattice. The energy of the electron is almost equal to that of the in-coming  $\gamma$ -ray, so the process produces projectiles capable of displacing atoms in the host lattice and causing radiation damage. Sosin refers to this process as "internal" electron irradiation, with the electron causing the Rutherford collision.

Collision mechanics shows that the electron of primary energy  $E_p$  can strike a host atom of mass  $M_2$  and transfer energy up to  $T_m$  to it, where  $T_m$  and  $E_p$  are related by

$$T_m = \frac{2 (E_p + m_e c^2) E_p}{M_2 c^2} \quad (1)$$

Here  $m_e$  is the mass of the electron and  $c$  is the velocity of light.

For situations relevant to our work, the energy of the incident  $\gamma$ -ray is transferred to electrons which dissipate it in the form of heat and of radiation damage through point defect production. In order for point defects to be produced,  $T_m$  must be greater than  $E_d$ , the energy to displace an atom from a normal lattice site, or in some cases it must be greater than  $E_r$ , the energy to replace one lattice atom with another. The displacement mechanism of point defect creation requires that a struck atom or "knock-on" force its way through neighboring atoms and into an interstitial site.

In addition, in certain cases a Compton electron directs a knock-on directly toward a nearest neighbor, which the knock-on replaces in the lattice and directs in turn toward its nearest neighbor. In these situations, the displacement propagates down a chain until the process ends with the creation of an interstitial at a lattice discontinuity. The vacancy at the beginning of the

chain along with the interstitial at the discontinuity form a separated Frenkel pair. This replacement mechanism of point defect production requires energy  $E_r$  about  $0.1 E_d$ , and Chadderton shows that about five replacement pairs will be produced for each displacement pair.

Since a 1 MeV  $\gamma$ -ray produces an electron of energy about 1 MeV, equation (1) indicates that energy  $T_m$  of 50 to 100 eV can be imparted to an atom in a typical engineering alloy. Since  $E_d$  is of order 10 eV, this energy is sufficient to produce one or two displacement Frenkel pairs or several more replacement pairs. It is apparent then that the radiation damage from  $Co^{60}$   $\gamma$ -irradiation should consist largely of single or small multiple interstitials and vacancies distributed throughout the lattice. One obvious effect of irradiation on morphology is the enhancement of solute diffusion by these excess vacancies.

Further, it is reasonable to assume that the binding energy of a solute atom in the precipitate is of order 10 eV, so that either "knock-ons" or electrons can also be expected to sputter atoms from the surface of precipitate particles. Moreover, the precipitate presents a natural termination point for a displacement propagation down a replacement chain in the lattice, so that a higher concentration of matrix vacancies or of solute atoms dissolved from precipitates can be expected at the periphery of the particle.

In short, based on the usual models of radiation damage, there is no reason to neglect the possibility that  $\gamma$  -irradiation damage is capable of causing changes in second phase morphology in a multiphase alloy.

## Rutherford Collision Damage in Multiphase Alloys

Because most basic experimental radiation damage studies are made in pure materials, there are few theoretical treatments of the effect of irradiation on second phase particles. A fairly recent review by Damask<sup>7</sup> summarizes the literature on this topic and indicates that five precipitate-related processes can occur when non-fissionable alloys are irradiated. They are: destruction of order; change of precipitate size; enhanced nucleation; enhanced diffusion; retarded diffusion. Damask concludes that electron and  $\gamma$ -irradiation should influence only the last two processes.

A more recent paper by Nelson<sup>8</sup> et al similarly classifies three simultaneously-occurring processes which can influence precipitate morphology. The first is recoil dissolution or the sputtering of atoms off precipitates by high energy particles. The second is disordering dissolution in which impinging particles destroy order on the periphery of an ordered precipitate and cause it to dissolve. The third is enhanced diffusion due to excess vacancies generated during irradiation. The authors, conclude (without experimental evidence) that only the last process will be operative in  $\gamma$  or electron irradiation.

Nelson et al consider the net effect of irradiation on spherical, ordered precipitates of volume  $V = 4\pi r^3/3$ . There are  $N$  atoms per unit volume in the precipitates, and each atom can be displaced by irradiation at a damage rate of  $K$  displacements/atom/sec.

The precipitates grow or shrink by a vacancy diffusion mechanism. The normal diffusivity  $D$  can be supplemented with an enhanced diffusivity  $D'$ , which comes about as radiation-induced vacancies increase atom mobility. For materials of low dislocation density

$$D' = \lambda^2 \left[ \frac{K \cdot V \cdot S}{z} \right]^{1/2} \quad (2)$$

where  $\lambda$  is the jump distance,  $\nu_s$  is the solute (vacancy) jump frequency, and  $z$  is a recombination parameter  $\approx 1$ .

As far as the precipitates themselves are concerned, recoil dissolution sputters atoms into the matrix at a flux  $\eta \approx 10^{14}$  K/cm<sup>2</sup>/sec. The flux causes the precipitate to decrease in volume at a rate

$$\frac{dV}{dt} = - \frac{4\pi r^2 \eta}{N} \quad (3)$$

If the precipitate is ordered, the irradiation particles disorder a shell of thickness  $l$ , on the periphery. A fraction  $q$  of the atoms in the shell will leave the precipitate and dissolve in the matrix, a process characterized by the dissolution parameter  $\psi = l q$ . The rate of volume change due to this effect is

$$\frac{dV}{dt} = - 4\pi r^2 \psi K \quad (4)$$

The kinetics of the processes are defined by the diffusivity  $D'' = D + D'$ , which is employed in the three simultaneous differential equations which govern particle growth or shrinkage. The equations are

$$\frac{dV}{dt} = 3D'' C_2 r/p, \quad (5)$$

$$\frac{dr}{dt} = - \frac{\eta}{N} + \frac{3D'' C_1}{4\pi p r} - D'' r^2 n, \quad (6)$$

and

$$\frac{dr}{dt} = - \psi K + \frac{3D'' C_1}{4\pi p r} - D'' r^2 n. \quad (7)$$

Here  $C_1$  is the total solute content of the system,  $C_2$  is the matrix solute concentration,  $p$  is the atom fraction of solute in precipitates and  $n$  is the number of precipitates per unit volume.

Analytical solutions to the three equations show that the behavior of the system is very complicated. Depending on the values of the various parameters involved:

1. Precipitates below a critical size may grow, while those above that size may shrink, i.e., simultaneous coarsening and decoarsening may occur.

2. Re-resolution may so enrich the matrix in solute that nucleation of a fine dispersion of precipitates may be superposed on shrinkage and growth of larger precipitates.

In general, the system responds to irradiation in a much more complex fashion than is observed in typical thermal-mechanical treatments. However, the magnitude of change of precipitate size resulting from the processes described by equations 2 through 6 can be estimated from the equations themselves. Consider as the most typical example, Al-Cu alloys in which the precipitate responsible for maximum hardening<sup>8</sup>,  $\theta'$ , is an ordered platelet, tens of  $\text{\AA}$  thick and several hundred  $\text{\AA}$  in diameter. Represent the precipitate as a sphere of  $r = 10^{-6}$  cm and note that our internal friction measurements in Cu show that  $\text{Co}^{60}$   $\gamma$ -irradiation at a dose of  $1 \times 10^2$  rads/sec produces damage at a  $K = 2 \times 10^{-13}$  displacements/atoms/sec. For these precipitates, the recoil mechanism described by equation (3) produces a rate of volume change

$$\frac{dV}{dt} \approx 10^{-33} \text{ cm}^3/\text{sec} \text{ (recoil dissolution).}$$

This corresponds to a rate of radius change  $dr/dt$  of about  $10^{-11}$  cm/sec. For an irradiation time of 10 hours ( $3.6 \times 10^4$  sec), a

net radius change of  $10^{-8} - 10^{-9}$  cm can occur. Thus reasonable irradiations result in changes in the order of monolayer in the precipitate size.

The disordering dissolution mechanism requires that the dissolution parameter  $\psi = \lambda q$  be estimated. It is reasonable that a  $\gamma$ -induced electron can disorder a region  $\lambda$ , at least one atomic diameter ( $10^{-8}$  cm) in depth. Assuming further that the probability  $q$  of atom leaving the disordered region rather than moving to re-order it is 0.1, then  $\psi = 10^{-9}$  cm. For a precipitate of radius  $10^{-6}$  cm, equation (4) predicts

$$\frac{dV}{dt} = 10^{-38} \text{ cm}^3/\text{sec (disordering dissolution)}.$$

Since the GP zones in these alloys are ordered, a typical  $\gamma$ -irradiation treatment will remove an additional monolayer from the precipitates.

These relationships show that  $\gamma$ -induced electrons can bring about measurable changes in precipitate size. It remains to ask whether significant changes are possible kinetically i.e. whether  $D'$  is large enough to allow significant solute atom transport. Assuming that  $\lambda = 3 \times 10^{-8}$  cm and that  $v_s = 10^7$  /sec (both typical values) then equation (2) yields,

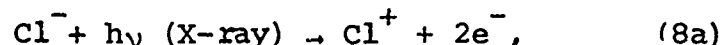
$$D' = 10^{-18} \text{ cm}^2/\text{sec (enhanced diffusion)}.$$

In his discussion of aging in Al-Cu, Fine<sup>10</sup> notes that  $D$  for Cu in Al at  $300^\circ\text{K}$  is  $10^{-25}$   $\text{cm}^2/\text{sec}$ , a value much too small to account for observed precipitation. He further mentions that excess vacancies introduced by quenching from the solutionizing temperature cause an enhanced diffusion coefficient  $D' = 10^{-18}$   $\text{cm}^2/\text{sec}$  to exist. This value is adequate to cause change in precipitate size at  $300-400^\circ\text{K}$ . Since  $D'$  due to quenching is of identical order of magnitude to that due to  $\gamma$ -irradiation, it can be concluded that favorable kinetic conditions exist for change of precipitate size during irradiation.

The theoretical predictions all indicate that  $\gamma$ -irradiation can influence microstructure, although conservative use of the predictions suggests that the influence will be very small. The following section of the literature review shows that the Coulombic repulsion of ions, ionized by high energy radiation, can bring about greater damage in multiphase materials than can the Rutherford collisions just considered.

#### Coulombic Repulsion Damage in Multiphase Alloys

In 1950, Varley<sup>11</sup> showed that the concentration of point defects produced in alkali halides by X-irradiation exceeded that predicted for Rutherford collisions by several orders of magnitude. He proposed that a much more significant cause of irradiation damage was the repulsion of like-charged ions created by X-rays. Specifically he noted the high probability of the reaction



followed by the dissociation of a small region in the alkali halide lattice through the Coulombic repulsion



where M denotes an alkali metal.

This type of reaction can occur only in poor electrical conductors, because the electrons created by the reaction (8a) remain detached from their parent ion for a time sufficient for displacement to occur only in poor conductors. In metals, the electrons immediately return to the parent ion, or free electrons in the metal electron "gas" rush to the ion so rapidly that the ion cannot be repelled from the equilibrium position by the like charges or its neighbors. It might be expected then that this Coulombic reaction can only cause radiation damage in metals which contain poorly-conducting second-phase particles; e.g. oxides, non-metallic inclusions or certain intermetallic compounds.



Ten years later, Platzman<sup>12</sup> showed that ionization and therefore, repulsion, might occur easily by the Auger effect in which impinging radiation increases the over-all energy of an atom to such an extent that electrons are emitted in a so-called "Auger-cascade." Loss of electrons causes the atom to become charged, and if the charge is of the same sign as that of neighboring ions, the parent ion is repulsed to an interstitial site, leaving a vacancy in the original position. Not only are point defects created by this mechanism, small precipitate particles can be literally shattered apart by Coulombic repulsion in certain cases.

Both the Varley and the Platzman mechanisms require that primary radiation dissipate its energy in causing electrons to be ejected from atoms rather than by causing secondary (fluorescent) radiation to be created. It can be shown<sup>13</sup> that the tendency of an irradiated atom to emit electrons rather than fluorescent radiation is proportional to  $[1 + (Z/30)^4]^{-1}$ , where  $Z$  is the atomic number. It is evident that the lighter the atom, the greater the ionization tendency, and the greater the susceptibility to radiation damage through Coulombic repulsion. This suggests that poorly-conducting second phase particles containing light atoms might be especially prone to radiation-induced morphology change.

In any event, it is evident that radiation damage theory predicts that the second phase particles in an engineering alloy can be influenced by  $\gamma$ -irradiation. The conventional "billiard-ball" collision mechanism can account for changes in precipitate size, shape, and number density, through enhanced diffusion, recoil dissolution, or disordering dissolution. The Coulombic repulsion mechanism can lead to dissolution of poorly-conducting second phase particles through either direct ionization (Varley) or Auger ionization (Platzman) events.

The next section of the report shows that internal friction provides an ideal tool for the study of these radiation damage processes, and the section following it describes the experimental results.

## EXPERIMENTAL RESULTS

### Damping Studies of Precipitation in Al-Cu

It is well known that internal friction measurements provide an extremely sensitive tool for the study of atomistic processes within solids, including recovery, radiation damage and precipitation. In a recently-published work<sup>14</sup> we have shown that ultrasonic pulse echo attenuation measurements in the MHz frequency range and resonance bar damping measurements in the kHz range allow accurate monitoring of the aging process in Al-3 Cu.

The pulse-echo method allows the measurement of the decay or attenuation ( $\alpha$ ) of a high frequency elastic wave pulse as it reverberates between parallel surfaces within a plate-like sample<sup>15</sup>. The resonance bar method, as conducted with the Marx<sup>16</sup> technique, allows the measurement of the energy loss or damping ( $\delta$ ) which occurs in a sample driven at resonance by quartz transducers. Both internal friction techniques are carried out with sample being aged and/or  $\gamma$ -irradiated in situ, and both allow measurement of modulus defect, another gauge of internal friction.

Figure 2 shows the behavior of ultrasonic attenuation and resonance bar damping during aging at 190°C of solution treated Al-3 Cu. Included in the figure is a plot of the Rockwell "E" hardness of the material as a function of aging time,  $t$ . It is seen that both techniques provide a sensitive gauge of the sub-microstructural and microstructural changes which occur during aging and which influence macroscopic properties.

In addition to yielding a direct qualitative measure of atomic processes taking place within the alloys, the measurements can be interpreted quantitatively so as to give insight as to the mechanisms responsible for the processes.

For example, Figure 2b shows  $\alpha$  as a function of  $t$  and frequency ( $f$ ). It is possible to divide  $\alpha(f, t)$  into the component

parts which each individual internal friction process contributes to the observed loss. A background loss  $\alpha_b(t)$ , which can be shown to be independent of  $t$ , arises because of extraneous effects and because of scattering by grain boundaries within the polycrystalline sample. A precipitate scattering loss  $\alpha_s(t)$ , which depends upon precipitate size and shape and is independent of  $f$  in these experiments, occurs as precipitates, even of those of sub-microstructural size, scatter the elastic wave. A dislocation loss  $\alpha_d$  arises because dislocations oscillate under the action of the vibratory elastic wave and dissipate energy. (Application of the Granato-Lucke<sup>17</sup> theory of dislocation damping to these experiments indicates that this latter loss should vary as  $f^2$  and consist of a time-dependent component  $\alpha_d(f^2, t)$  and a time independent component  $\alpha_d(f^2)$ .) The total attenuation is

$$a(f, t) = \alpha_b(f) + \alpha_d(f^2) + \alpha_s(t) + \alpha_d(f^2, t). \quad (9)$$

The time-dependent portion of the attenuation,  $\Delta\alpha$ , gives a measure of the kinetic processes occurring during aging and consists of a frequency-dependent dislocation contribution and a frequency-independent scattering contribution; thus

$$\Delta\alpha = \alpha(f, t) - [\alpha_b(f) + \alpha_d(f^2)] = \alpha_s(t) + \alpha_d(f^2, t) \quad (10)$$

Plots of  $\Delta\alpha$  versus  $f^2$  for various aging times should yield straight lines if this analysis is valid. The intercepts are equal to  $\alpha_s(t)$  and should give a direct measure of changing precipitate size and/or shape. The slopes should be proportional to the changing dislocation component of the internal friction as dislocations become either more pinned or more mobile as precipitates form and remove solute from the matrix.

Figure 3a shows such plots for aging times to 250 hours. They are indeed linear, with intercepts and slopes increasing

with  $t$ . Figure 3b shows the intercepts  $\alpha_g(t)$  plotted against independent measurements of G. P. zone diameter obtained as a function of  $t$ . The correlation between the two is evident.

Our damping studies of aging in the absence of radiation have shown that:

1. Change of precipitate size and/or shape can be followed and analyzed quantitatively by means of internal friction experiment and theory.

2. The change in the dislocation damping of an alloy undergoing structural change provides a gauge of the processes causing change, and insight regarding the mechanisms of the processes can be gained through application of damping theory.

### Irradiation-Damping Studies

Because the experiments just discussed have shown damping measurements to be a sensitive gauge of precipitation-related phenomena, the techniques have been applied to fully hardened Al alloys subjected to  $\gamma$ -irradiation in the 14 kilocurie  $\text{Co}^{60}$   $\gamma$  source of the University's radiation laboratory. Emphasis has been on the use of the Marx resonance bar technique, with polycrystalline rod samples vibrated at 80 kHz in the fundamental longitudinal mode.

Figure 4 shows the in situ damping of a 99.99% pure Al sample irradiated at a dose of  $I \times 10^2$  rads/sec. The sample was put through a heat treatment corresponding to the T6 condition for direct comparison with alloy samples. (Solution heated at 500°C, quenched, aged at 190°C for 10 hours.) The decrease in the damping noted has been observed often in single phase materials during electron and  $\gamma$ -irradiation. It is attributed to the decrease in the dislocation contribution to the internal friction, as the point defects created during irradiation migrate to dislocations, immobilize them, and eliminate their ability to oscillate and dissipate vibrational energy. The accompanying increase in resonance frequency  $f_r$  with decrease in damping is consistent with the relationship of modulus defect to damping. Stern and Granato<sup>18</sup> have conducted extremely detailed experiments in the  $\gamma$ -irradiation of single-phase materials and have provided detailed analysis of the damping results in terms of dislocation damping theory. Our observations are consistent with theirs and certainly are not surprising.

Figure 5 shows that high-purity Al - 3 W/o Cu in the T-6 condition responds to irradiation in a manner similar to pure Al, with a monotonic decrease in  $\delta$  and its corresponding increase in  $f_r$ . Both pure Al and the binary alloy then exhibit behavior consistent with the usual dislocation pinning model of irradiation - damping experiments.

On the other hand, surprising results are obtained during  $\gamma$ -irradiation of commercially pure 2017-T6 and 2024-T6, Figures 6 and 7. The usual decrease in  $\delta$  is observed during the first 7 hours of irradiation, presumably because radiation-induced point defect pinners are immobilizing dislocations. At longer times however,  $\delta$  begins to increase and approach a saturation value. The decrease in  $f_r$  which should accompany the unusual increase in  $\delta$  is observed.

Table I lists the nominal compositions of the commercial alloys. One major difference between them and the pure Al or the Al - Cu binary alloy is the presence of Mg, which is a light

Table I

Nominal Compositions of Commercial Al Alloys

Alloy	Wt% Cu	Wt% Mg	Wt% Mn
2017	4.0	0.5	0.5
2024	4.5	1.5	0.5

element and an extremely potent oxide former. This suggests that Mg - bearing alloys might be especially susceptible to radiation damage by way of the Varley-Platzmann mechanism.

In order to determine if the presence of Mg is related to the anomalous damping minimum observed in the commercial alloys. Measurements have been conducted on a high purity binary Al - 9.5 W/o Mg

donated by ALCOA. The alloy, which is known to age harden sluggishly is solution-treated at 530° C for 2 hours, quenched and aged at 190° C for 12 hours. Its damping is then determined in situ during irradiation with the Marx gauge. Figure 8 shows that indeed, a damping minimum appears after 4 hours of  $\gamma$ -irradiation, indicating that the unusual behavior is somehow associated with Mg.

One major disadvantage of the damping measurements summarized in Figures 4 through 8 is that they are indirect and do not give a clear indication of the effect of irradiation on precipitate morphology. For that reason, transmission electron micrographs of both the unirradiated and irradiated materials have been obtained.

Figure 9 shows pure Al in the as-heat treated condition and after 7 and 25 hours of  $\gamma$ -irradiation. The original appearance is that of a single phase material of low dislocation density. After 7 hours of irradiation, small spots, which are probably radiation-induced dislocation loops, appear in the microstructure, and their density increases during subsequent irradiation to 25 hours.

It might be expected that the loops, which increase dislocation density, could cause an increase in dislocation damping. This is evidently not the case since Figure 4 shows a monotonic decrease in  $\delta$  during irradiation. The micrographs along with the damping data shows that pure Al has a very predictable response to irradiation.

The microstructure of Al - 3 Cu in the T6 condition as shown in Figure 10 after 0, 7 and 25 hours of irradiation are quite similar. The precipitates are flat plates of a general square shape,



about  $1000 \text{ \AA}$  in long dimension and roughly  $10 \text{ \AA}$  thick. The size, shape and number density of particles remain unchanged during irradiation, and this is consistent with the damping data which show the steady decrease in  $\delta$  characterizing simple dislocation pinning.

Both Figures 9 and 10 then indicate that no significant microstructural changes occur when the unusual minimum in damping is absent. Figure 11 shows electron micrographs of 2017-T6 after 0, 7 and 25 hours of irradiation. The as-age hardened structure consists of a profuse distribution of fine precipitates in the matrix. The high precipitate number density of  $6 \times 10^{10}$  per  $\text{cm}^2$  is to be expected for a commercial alloy, designed to show marked strengthening. After 7 hours of irradiation, a time corresponding to the minimum in  $\delta$ , precipitate coarsening occurs. The 25 hour irradiation produces a fine dispersion of precipitates similar to the original one. The combined coarsening-decoarsening predicted by Nelson et al. has taken place, and is characterized by the internal friction minimum.

The damping minimum also appears in the Al - 9.5 Mg alloy, whose microstructure is shown in Figure 12. The unirradiated but age-hardened material shows little evidence of precipitation. This is consistent with the known sluggishness of precipitation in this binary alloy.<sup>19</sup> Little if any change in microstructure is observed after 4 hours of irradiation, the time working the minimum in  $\delta$ . After 25 hours of irradiation however, a time adequate for the damping to pass through the minimum and return to a high value, a profuse precipitation of fine discs is observed. Once again it is seen that the damping minimum is an indicator of radiation-induced morphological changes.

Thus far it has been seen that radiation damage theory, based on either Rutherford collision or Coulombic repulsion models, predicts that  $\gamma$ -irradiation can influence the microstructure of a multiphase alloy. Further both damping measurements and electron microscopy indicate that change can be brought about in certain Al alloys.

## CONCLUSIONS

The INTRODUCTION to this report sets three major experimental objectives. The first is to establish whether  $\gamma$ -irradiation can cause morphology change. The second is to explain the reason that irradiation influences morphology. The third is to develop suggestions for the control of material behavior in a  $\gamma$ -irradiation environment. The first objective has been met with good success, and the second and third have been partially met.

### The Existence of an Effect

Both Rutherford collision and Coulombic repulsion theory indicate that  $\gamma$ -irradiation should influence the size, shape and distribution of precipitates in multiphase alloys. The respective theories are not clear as to the extent of the influence, but first estimates suggest that the effect should be small. Usual treatments of radiation damage, in fact, completely neglect  $\gamma$ -irradiation damage as being capable of exerting significant effects on structure and properties. The damping and microscopy results show independently that microstructural changes do occur.

The increase in  $\delta$  after a critical period of irradiation may be logically attributed, at first thought, to the increase in dislocation density in the materials as radiation-induced dislocation loops are formed. This explanation is inadequate however because neither pure Al or Al - 3 W/O Cu show the minimum although there is evidence that loops are forming.

The internal friction minimum can only be interpreted in terms of a net freeing of dislocations of solute atom pinners after a critical irradiation dose. This implies a net transfer of solute atoms from Cottrell atmospheres into the matrix or into precipitates.

The electron micrographs indicate that the transfer is into precipitates since second phase morphology changes after the critical irradiation dose. There is no doubt that  $\gamma$ -irradiation changes the microstructure of certain of these materials.

#### Mechanisms of the Effect

The reasons behind the observed effects are not evident. Enhanced diffusion and nucleation may be playing a part in the kinetic processes. Direct shrinking of precipitates because of Rutherford collisions may be occurring. Precipitate break-up because of Coulombic effects may be taking place. More in-depth studies in systems with alloying elements of a range of Z and oxide-forming tendencies are necessary. Further kinetic studies yielding the time dependence of precipitate growth and/or shrinkage are necessary to establish the roles of enhanced diffusion or nucleation.

#### Property Control in a $\gamma$ -Irradiation Environment

At this point in the investigation it is evident that Mg plays an important part in an alloy's susceptibility to  $\gamma$ -irradiation damage. Its presence should be avoided until such time that the clear relationship between structure, properties and  $\gamma$ -irradiation in these alloys is determined.

## REFERENCES

1. S. D. Harkness and C. Y. Li, "Theoretical Study of Swelling of Fast Neutron-Irradiated Materials," Argonne National Laboratory, Report 7588 (1969).
2. C. Cawthorne and E. J. Fulton, *Nature*, 216 757 (1967).
3. C. F. Bilsby and J. Standring, "Neutron Irradiation and Coarsening Kinetics of  $\gamma'$ ", " TRG Report 2113, 1971.
4. L. T. Chadderton, Radiation Damage in Crystals, (John Wiley, New York, 1965).
5. A. Sosin, *Adv. in Mats. Res.* 2, 159 (1968).
6. O. S. Oen and D. K. Holmes, *J. Appl. Phys.*, 30, 1289 (1959).
7. A. C. Damask in Radiation Effects, W. F. Sheely ed. (Gordon and Breach, New York, 1967) p. 77.
8. R. S. Nelson, J. A. Hudson, and D. J. Mazey, "Stability of Precipitates in an Irradiation Environment," AERE Report R7120, 1972.
9. J. M. Silcock, T. J. Heal, and H. K. Handy, *J. Inst. Met.* 82, 239 (1953).
10. M. Fine, Intro. to Phase Transformations, (MacMillan, New York, 1964) p. 109.
11. J. H. O. Varley, *J. Nuc. Energy*, 1, 130 (1954).
12. J. Durup and R. L. Platzman, *Disc. Far. Soc.* 31, 156 (1961).
13. E. V. Candon and H. Odishaw in Handbook of Physics, (McGraw-Hill, New York, 1958), p. 124.
14. N. F. Fiore and S. K. Gupta, *Met. Trans.*, 2, 1065 (1971).
15. R. Tuell, C. Elbaum, and B. Chick, Ultrasonic Methods in Solid State Physics, (Academic Press, New York, 1969).
16. J. Marx, *Rev. Sci. Instr.*, 22, 503 (1951)
17. A. Granato and K. Lücke, *J. Appl. Phys.*, 27, 583 (1956).

18. R. M. Stern and A. Granato, *Acta Met.*, 10, 358 (1962).
19. A. Kelly and R. B. Nicholson, *Prog. in Mat. Sci.*, 10, 151 (1962).

## LIST OF FIGURES

- Figure 1. Toughness of 2017-T6 as a function of  $\text{Co}^{60}$   $\gamma$ -irradiation dose.
- Figure 2. Sensitivity of internal friction measurements to microstructural changes in Al-3 w/o Cu.
- Figure 3. Analysis of ultrasonic measurements of aging of Al-3 w/o Cu at  $190^{\circ}\text{C}$ .
- Figure 4. Effect of  $\gamma$ -irradiation on damping ( $\delta$ ) and resonance frequency (fr) of 99.99% pure Al.
- Figure 5. Effect of  $\gamma$ -irradiation on damping ( $\delta$ ) and resonance frequency (fr) of Al-3 w/o Cu.
- Figure 6. Effect of  $\gamma$ -irradiation on damping ( $\delta$ ) and resonance frequency (fr) of 2017-T6.
- Figure 7. Effect of  $\gamma$ -irradiation on damping ( $\delta$ ) and resonance frequency (fr) of 2024-T6.
- Figure 8. Effect of  $\gamma$ -irradiation on damping ( $\delta$ ) and resonance frequency (fr) of Al-9.5 w/o Mg.
- Figure 9. Electron micrographs of 99.99% Al after 0, 7 and 25 hours of  $\gamma$ -irradiation.
- Figure 10. Electron micrographs of Al-3 w/o Cu after 0, 7 and 25 hours of  $\gamma$ -irradiation.
- Figure 11. Electron micrographs of 2017-T6 after 0, 7 and 25 hours of  $\gamma$ -irradiation.
- Figure 12. Electron micrographs of Al-9.5 w/o Mg after 0, 4 and 25 hours of  $\gamma$ -irradiation.

Table I

Table I      Nominal Compositions of Commercial Al Alloys

SEE PAGE 17

**Preceding page blank**



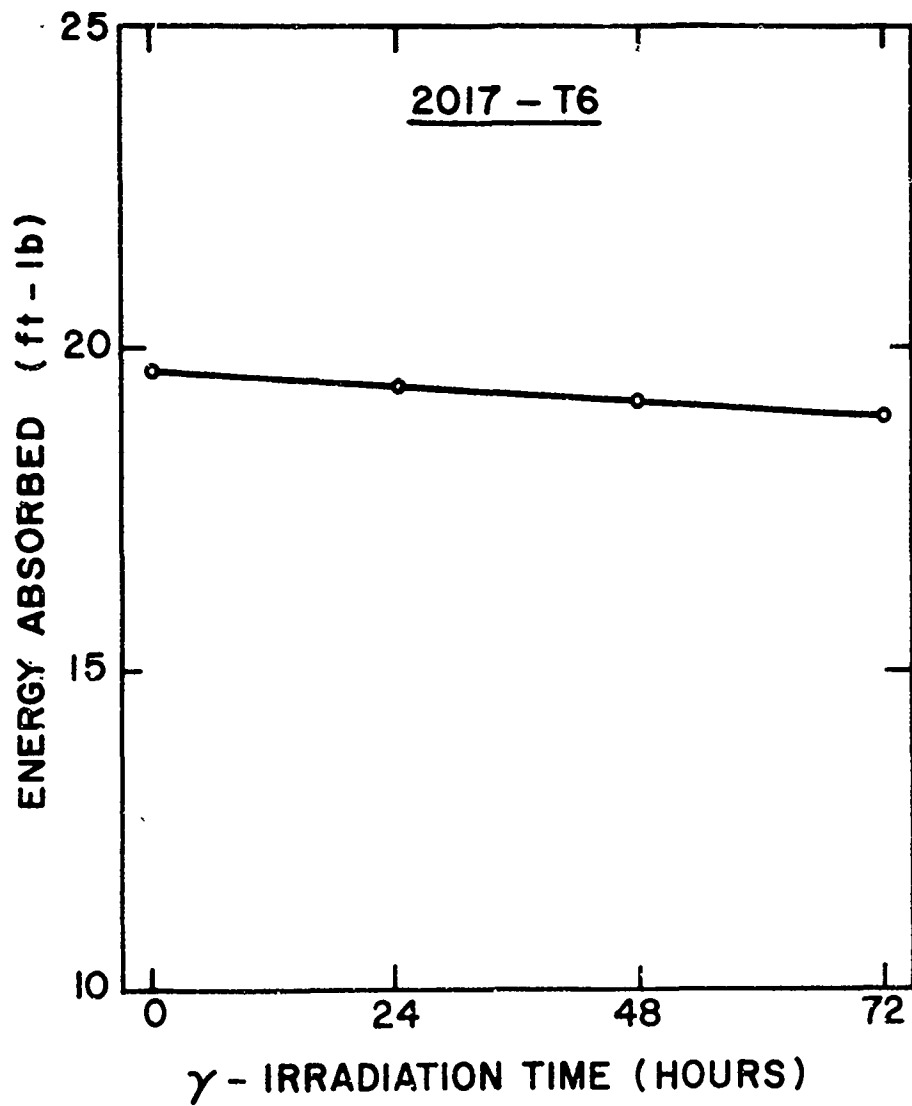
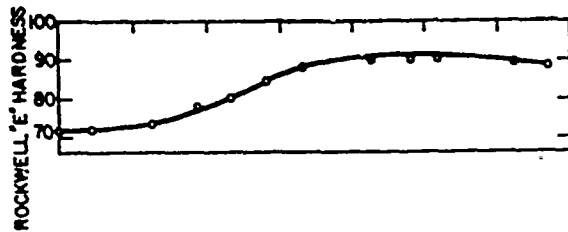
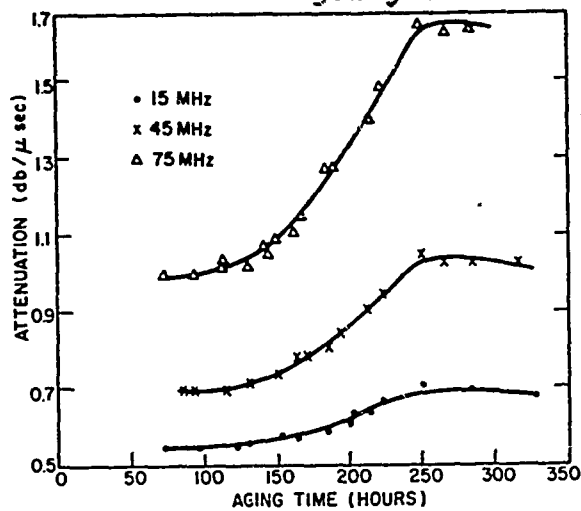


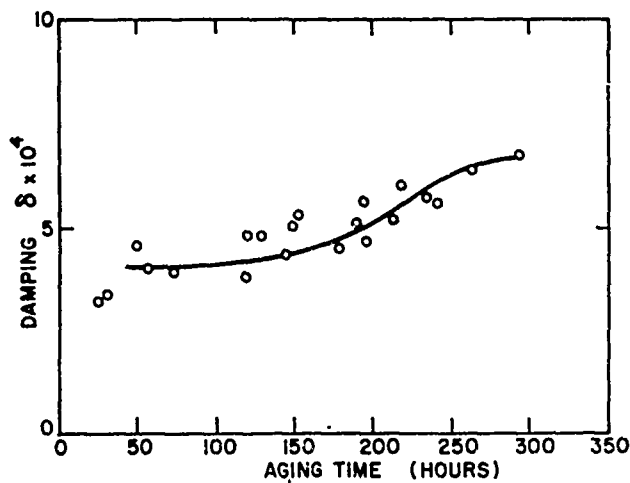
Figure 1. Toughness of 2017-T6 as a function of  $\text{Co}^{60}$   $\gamma$ -irradiation dose. (Each point represents average value of 5 impact tests).



2a. Rockwell E hardness versus ageing time at 190°C.

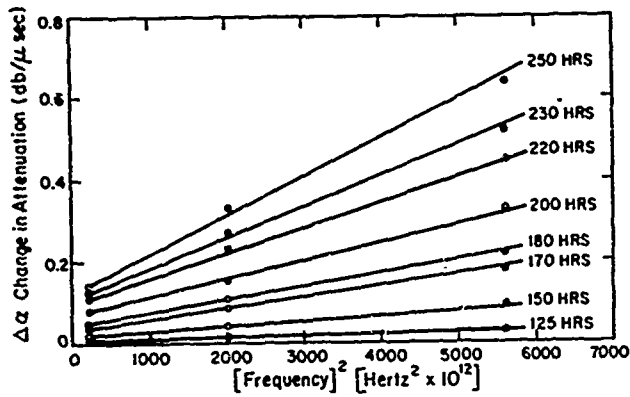


2b. Ultrasonic attenuation versus ageing time at 190°C.

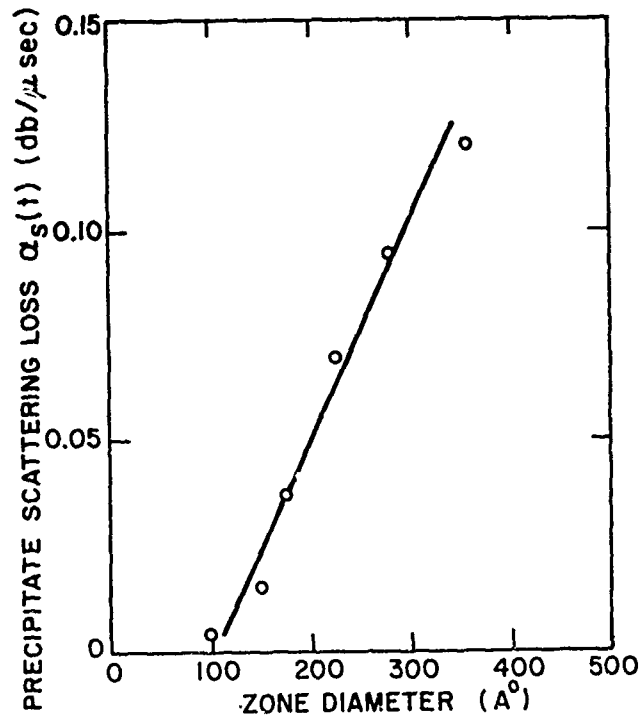


2c. Resonance bar damping versus ageing time at 190°C.

Figure 2. Sensitivity of internal friction measurements to microstructural changes in Al - 3 w/o Cu.



3a. Separation of dislocation damping and precipitate scattering components of ultrasonic attenuation.



3b. Attenuation due to precipitates versus precipitate size.

Figure 3. Analysis of ultrasonic measurements of ageing of Al - 3 w/o Cu at 190°C.

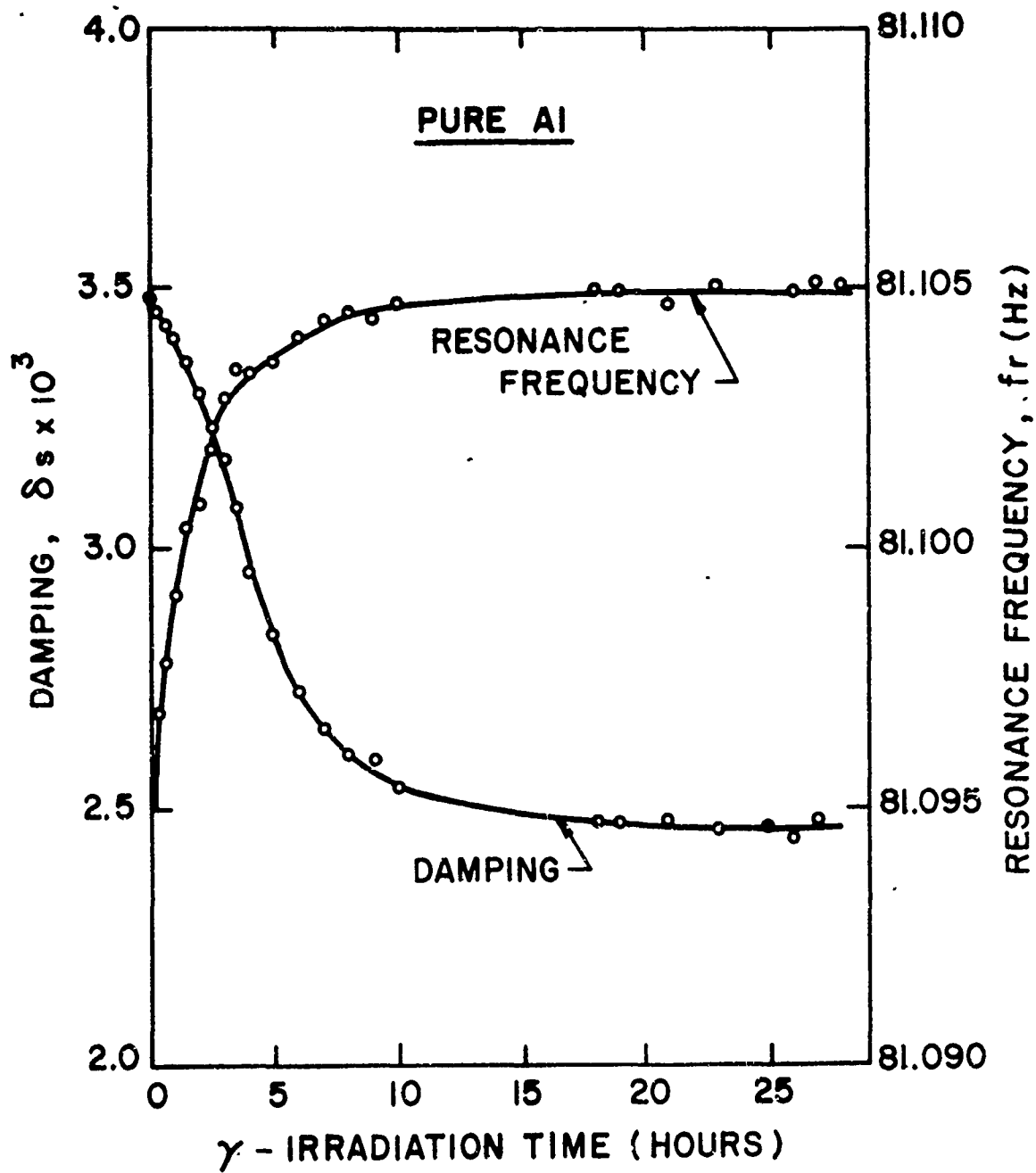


Figure 4. Effect of  $\gamma$ -irradiation on damping ( $\delta$ ) and resonance frequency ( $f_r$ ) of 99.99% pure Al.

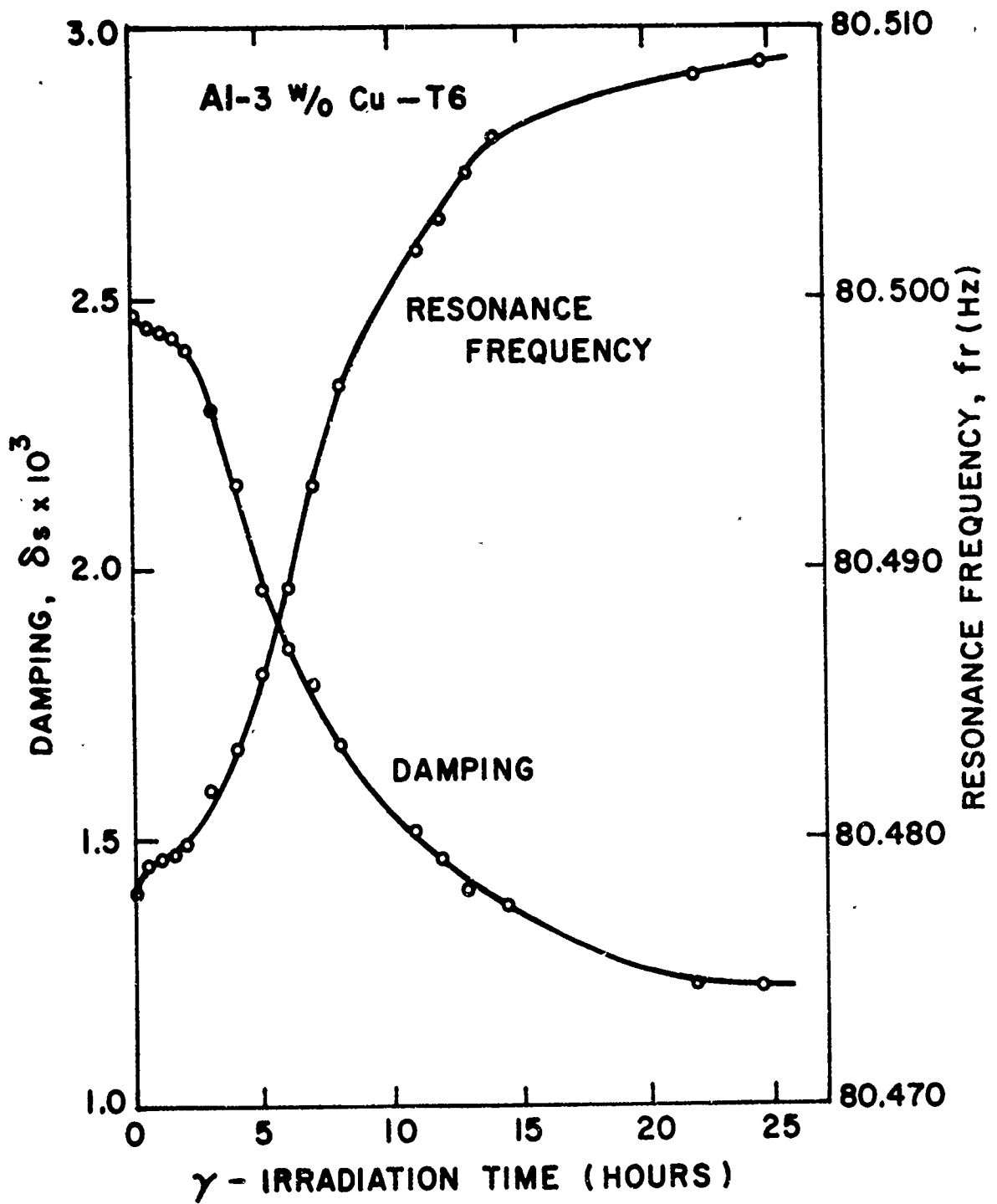


Figure 5. Effect of  $\gamma$ -irradiation on damping ( $\delta$ ) and resonance frequency ( $f_r$ ) of Al-3 w/o Cu.

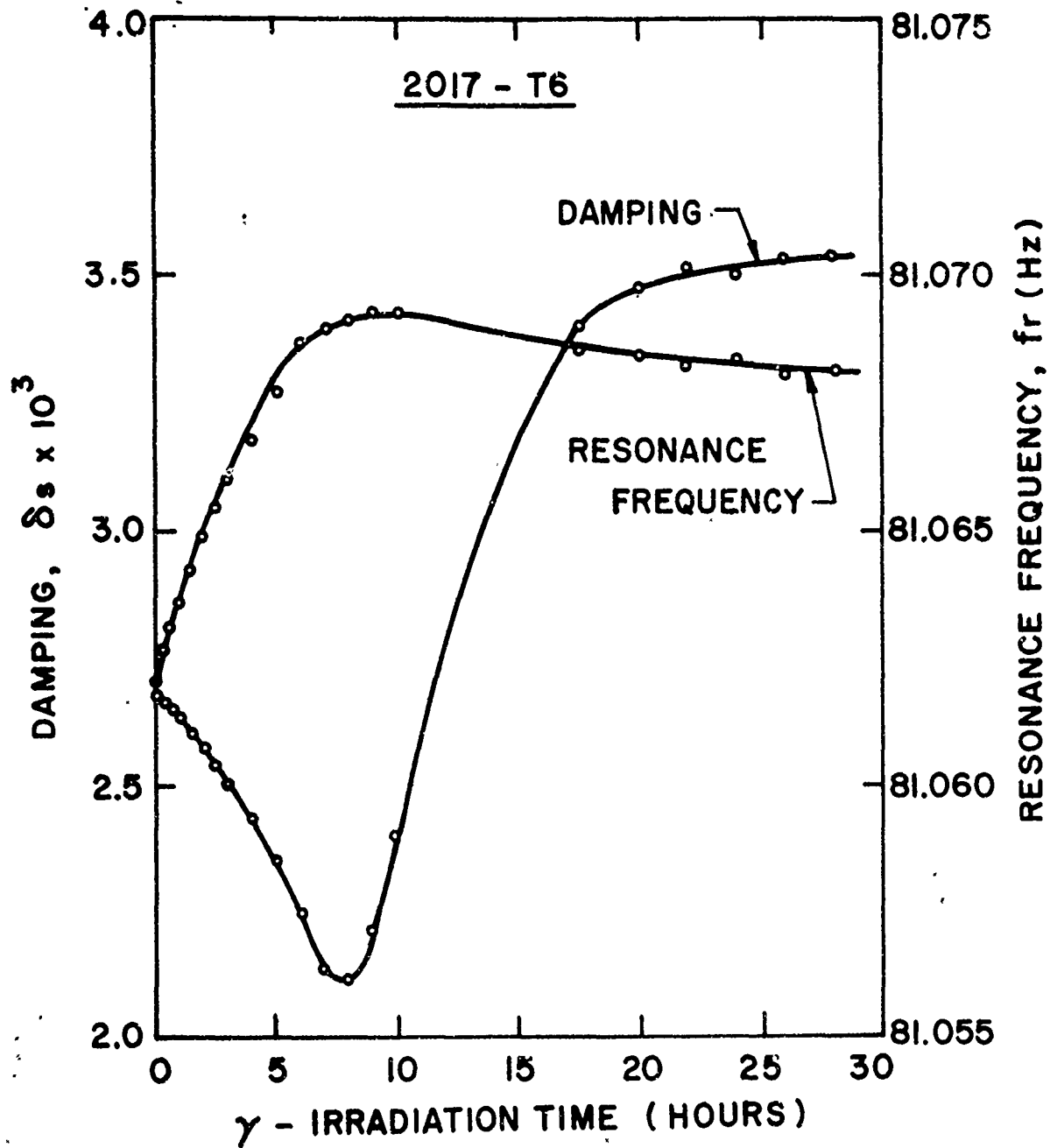


Figure 6. Effect of  $\gamma$ -irradiation on damping ( $\delta$ ) and resonance frequency ( $f_r$ ) of 2017-T6.

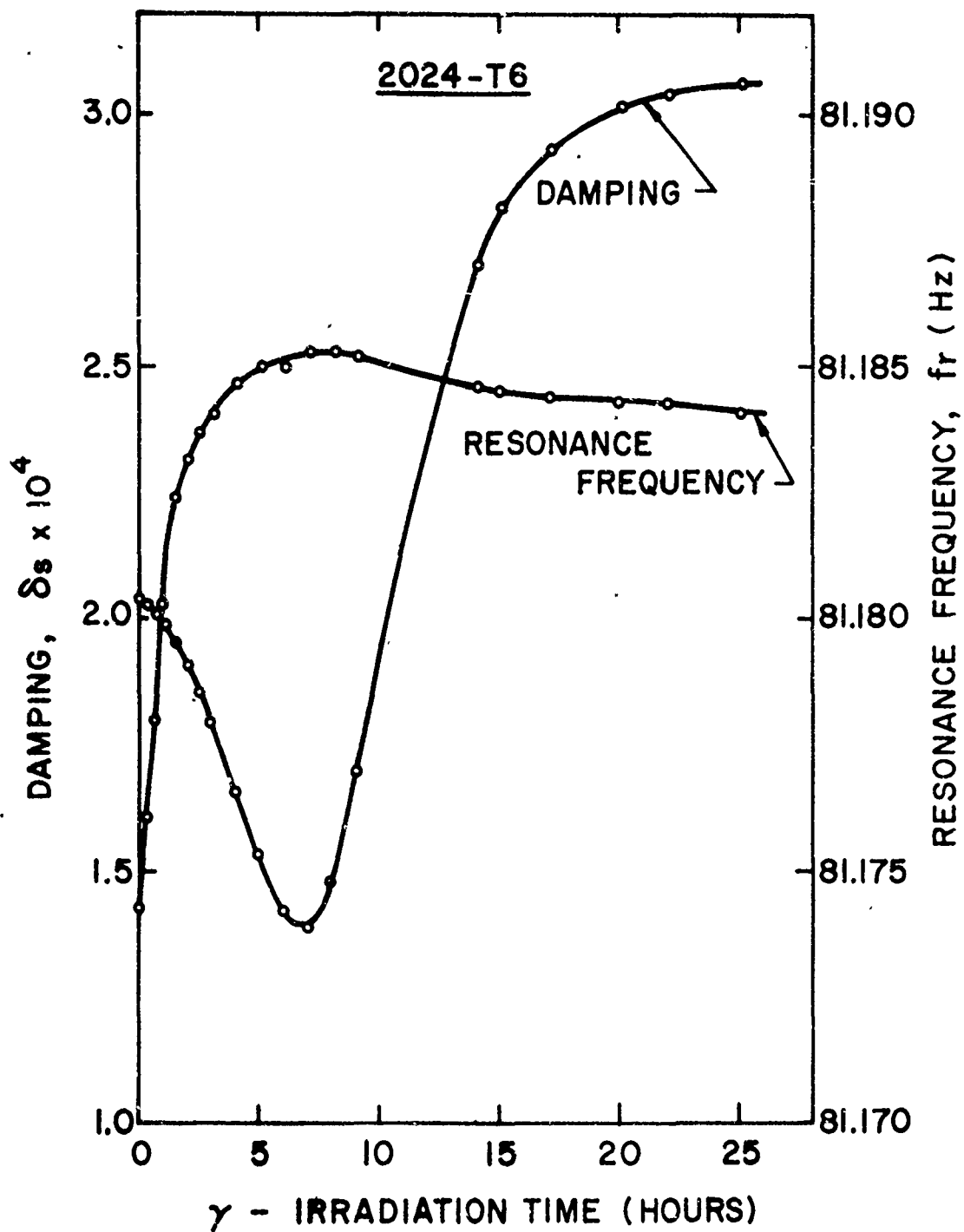


Figure 7. Effect of  $\gamma$ -irradiation on damping ( $\delta$ ) and resonance frequency ( $f_r$ ) of 2024-T6.

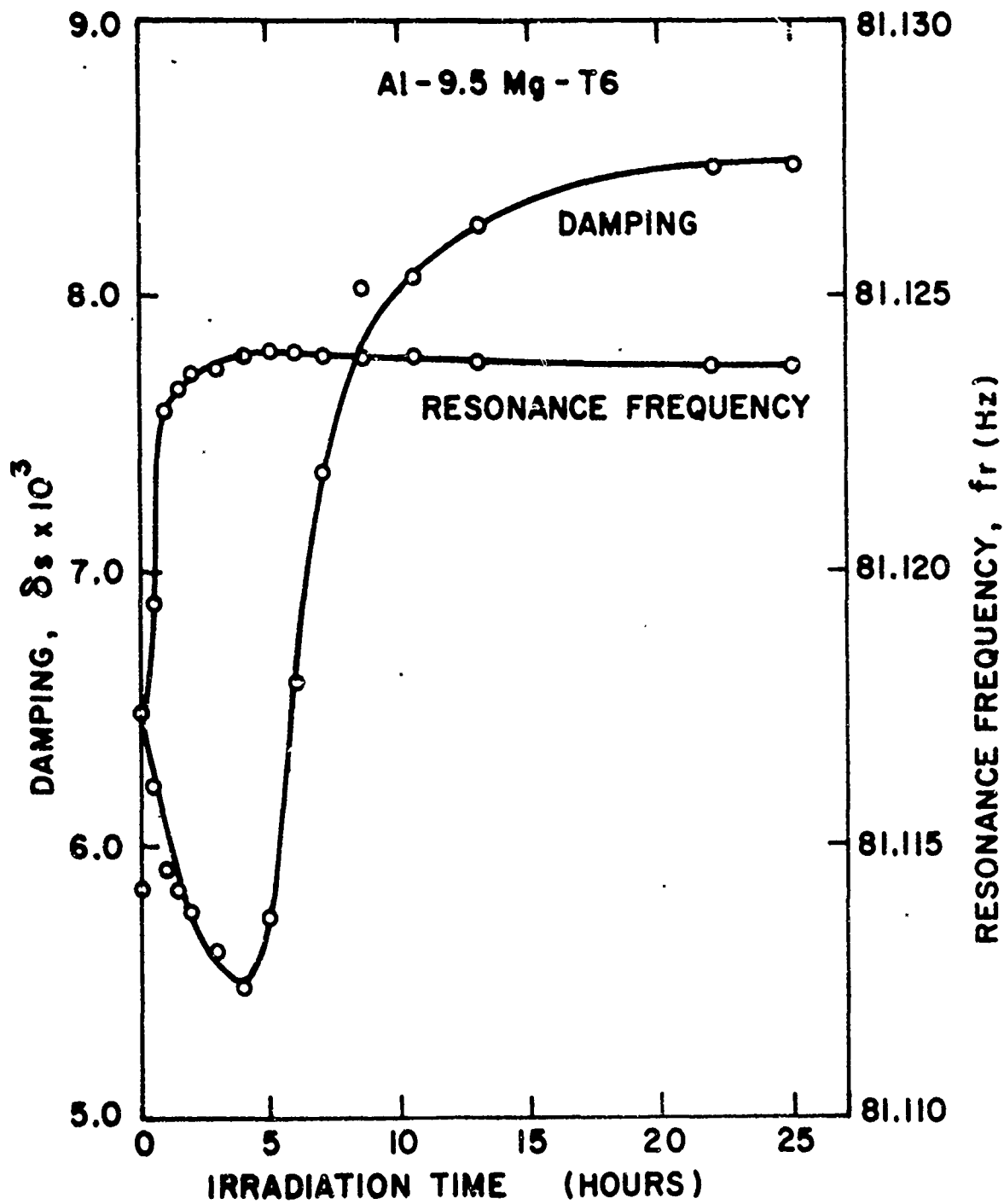
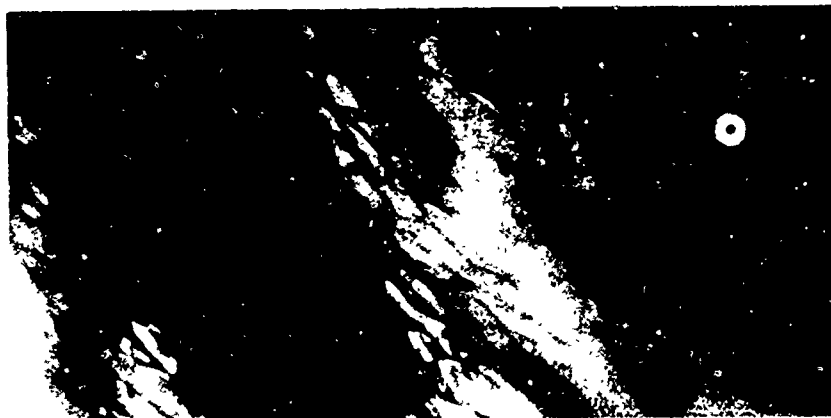


Figure 8. Effect of  $\gamma$ -irradiation on damping ( $\delta$ ) and resonance frequency ( $f_r$ ) of Al-9.5 w/o Mg.



Figure 9



(a) 99.99% Al. Unirradiated



(b) 99.99% Al. Irradiated 7 hours at a  $\text{Co}^{60}$   $\gamma$  dose of  $6 \times 10^3$  rad/min.

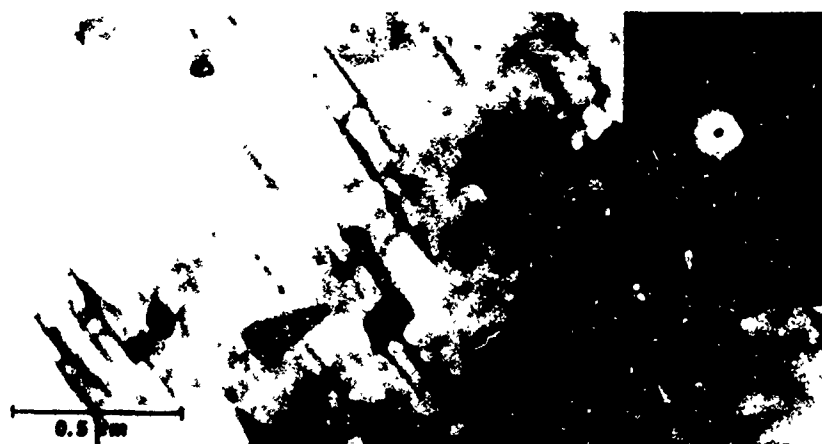


(c) 99.99% Al. Irradiated 25 hours at a  $\text{Co}^{60}$   $\gamma$  dose of  $6 \times 10^3$  rads/min.

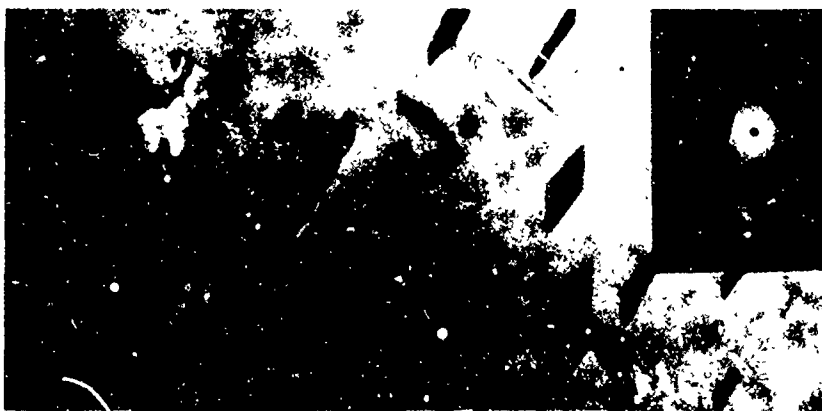
Figure 10



(a) Al-3 w/o Cu. Unirradiated.



(b) Al-3 w/o Cu. Irradiated 7 hours at a  $\text{Co}^{60}$   $\gamma$  dose of  $6 \times 10^3$  rads/min.



(c) Al-3 w/o Cu. Irradiated 25 hours at a  $\text{Co}^{60}$   $\gamma$  dose of  $6 \times 10^3$  rads/min.

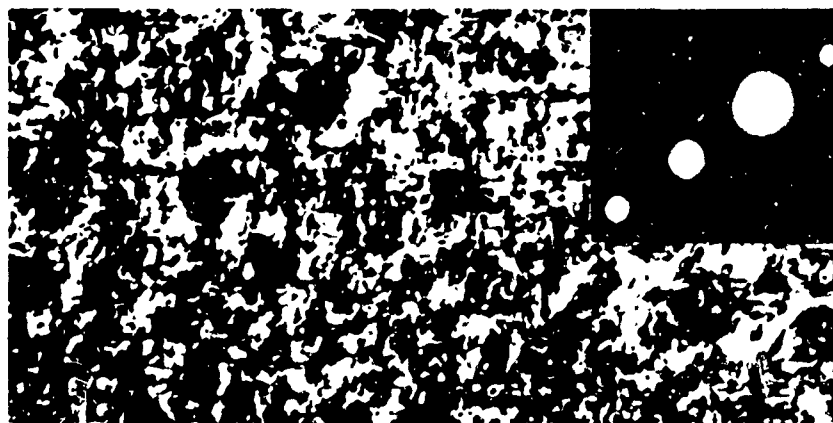
Figure 11



(a) 2017-T6 Unirradiated.



(b) 2017-T6 Irradiated 7 hours at a  $\text{Co}^{60}$   $\gamma$  dose of  $6 \times 10^3$  rads/min.



(c) 2017-T6 Irradiated 25 hours at a  $\text{Co}^{60}$   $\gamma$  dose of  $6 \times 10^3$  rads/min.

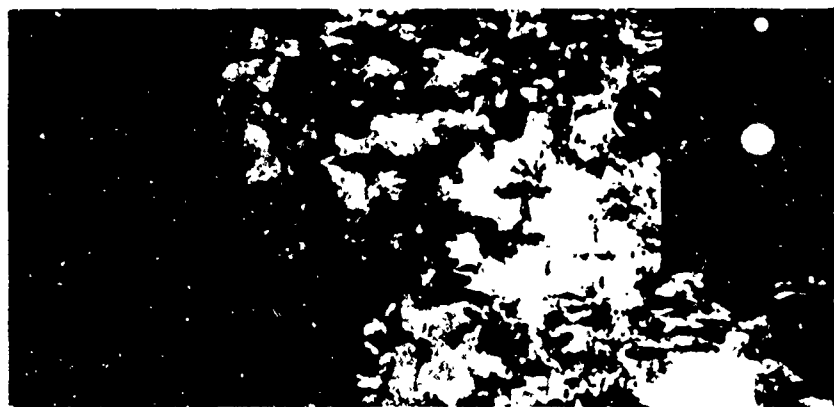
Figure 12



(a) Al-9.5 w/o Mg. Unirradiated.



(b) Al-9.5 w/o Mg. Irradiated 4 hours at a  $\text{Co}^{60}$   $\gamma$  dose of  $6 \times 10^3$  rads/min.



(c) Al-9.5 w/o Mg. Irradiated 25 hours at a  $\text{Co}^{60}$   $\gamma$  dose of  $6 \times 10^3$  rads/min